Pedosphere **19**(): 1–, 2009
ISSN 1002-0160/CN 32-1315/P

Published by Elsevier Limited and Science Press

PEDOSPHERE

www.elsevier.com/locate/pedosphere

Mobility of Arsenic and Heavy Metals in a Sandy-Loam Textured and Carbonated Soil*[1]

I. GARCÍA[1], M. DIEZ[2], F. MARTÍ N[2,*2], M. SIMÓN[1] and C. DORRONSORO[2]

[1]*Departamento Edafología y Química Agrícola. CITE IIB. Carretera Sacramento s/n, 04120, University of Almería (Spain). E-mail: inesgar@ual.es*
[2]*Departamento Edafología y Química Agrícola. Campus Fuentenueva s/n, 18002, University of Granada (Spain)*

(Received , 200 ; revised , 200)

ABSTRACT

The continued effect of the pyrite-tailing oxidation on the mobility of arsenic, lead, zinc, cadmium, and copper was studied in a carbonated soil under natural conditions, with the experimental plot preserved with a layer of tailing covering the soil during three years. The experimental area is located in Southern Spain and was affected by a pyrite-mine spill. The climate in the area is typically Mediterranean, which determines the rate of soil alteration and element mobility. The intense alteration processes that occurred in the soil during three years caused important changes in its morphology and a strong degradation of the main soil properties. In this period, lead concentrated in the first 5 mm of the soil, with concentrations higher than 1 500 mg kg^{-1}, mainly associated to the neoformation of plumbojarosite. Arsenic was partially leached from the first 5 mm and mainly concentrated between 5–10 mm in the soil, with maximum values of 1 239 mg kg^{-1}; the retention of arsenates was related to the neoformation of iron hydroxysulfates (jarosite, schwertmannite) and oxyhydroxides (goethite, ferrihydrite), both with a variable degree of crystallinity. The mobility of Zn, Cd, and Cu was highly affected by pH, producing a stronger leaching in depth; their retention was related to the forms of precipitated aluminium and, in the case of Cu, also to the neoformation of hydroxysulfate.

Key Words: arsenic, heavy metals, oxidation, pyrite-tailing, soil

Citation: García, I., Diez, M., Martín, F., Simón, M. and Dorronsoro, C. 2009. Mobility of arsenic and heavy metals in a sandy-loam textured and carbonated soil. *Pedosphere.* **19**(): – .

INTRODUCTION

The oxidation of sulfide minerals is a complex biogeochemical process that involves hydration, oxidation, and hydrolysis reactions, resulting in the transformation of sulfides into sulfates, the generation of acidic conditions, and the solubilization of elements (Singer and Stumm, 1970; Förstner and Wittmann, 1983; Nordstrom, 1982).

Although the reaction is complex, the final products are sulfates, iron in oxidized forms, and a strong acidification of the medium; a simplified equation of natural pyrite alteration/oxidation was given by Stumm and Morgan (1981).

$$4\ FeS_{2(s)} + 15\ O_2 + 14\ H_2O \leftrightarrow 4\ Fe(OH)_{3(s)} + 8\ SO_4^{-2} + 16\ H^+ \quad (1)$$

Where subscript (s) represents solid phase.

All the reactions involved in this process can be influenced by the presence of bacteria (*e.g.*, *Thiobacillus ferroxidans*) and the variation in the redox conditions, strongly affecting the normal oxidation rates (Lacey and Lawson, 1979; Bigham and Nordstrom, 2000). The products of this reaction are common in acid mine drainages, and the interaction of these solutions with soil and sediments results in the mobilization of a great number of elements coming from mineral dissolutions (Karathanasis *et al.*, 1988;

*[1]Project supported by the Science and Technology Ministry of Spain (No. REN 2003-03615).
*[2]Corresponding author. E-mail: fjmartin@ugr.es.

Karathanasis and Thompson, 1995; Nordstrom and Alpers, 1999; Monterroso and Macías, 1998). These elements may enter and distribute themselves in the environment through superficial waters, contaminating soils and surrounding terrestrial ecosystems and producing a toxicity risk of more sensitive media (plants, animals, and human beings) (Holub *et al.*, 1993).

When the acidic solution infiltrates into the soil, the generated protons react with the main constituents of the soil; a partial neutralization is produced by the cations of the exchangeable complex of the soil and by the primary minerals (mainly silicates), and a stronger neutralization occurs if carbonate minerals are present (Cravotta and Trahan, 1999). After these reactions, an increase in pH occurs, and the solubility of dissolved elements is reduced mainly by reactions of precipitation, coprecipitation, or adsorption in the exchangeable complex of the soil (Xu *et al.*, 1997).

In this work, we studied, under natural conditions, the effect of a pyrite-tailing spill over a carbonate soil three years after an accident that covered the soils with tailings and acidic water. The main pollutants involved were As, Pb, Zn, Cu, and Cd, with high concentrations in sulfur and iron. The subsequent drying and aeration of the tailings deposited over the soils resulted in an intense and rapid oxidation of the sulfides and a substantial increase in the concentration of potentially toxic elements that intensely affected the involved soils (Simón *et al.*, 2001). The potential risk of this contamination process and the possibility of mobilizing the elements into the ecosystem towards other superficial or subsuperficial medium (*e.g.*, groundwater) have very important environmental implications that must be studied under natural conditions.

In previous investigations (Dorronsoro *et al.*, 2002; Simón *et al.*, 2002), these processes in carbonate soils in short-term were studied in detail (2 and 15 months after the spill, respectively). These studies focused in the processes that related both to the changes in the soil properties and constituents of the area and to the mobility and retention of the contaminant elements in relation to the mineralogical changes occurred in the same soil type and area.

The present study was performed to assess the mobility of arsenic, lead, zinc, cadmium, and copper released after the oxidation of the tailings deposited in the carbonate soil (previously studied in short-term); but, in this case, three years after the accident, the detailed soil sampling performed (millimetric scale) allows us to identify more accurately the distribution of these elements in depth in the profile and to study the adsorption and precipitation processes that had occurred in the soil.

MATERIALS AND METHODS

In the area affected by the spill of pyrite tailings, two plots have been preserved (0743320–4125595; 0743396–4125796 UTM (Universal Transverse Mercator) coordinates) in the location known as *Vado del Quema* (Seville, southern Spain), without carrying out any remediation measure; the layer of pyrite tailings covering the soil surface has been maintained till today.

The climate of the area is typically Mediterranean, with a mean annual rainfall of 613 mm, a mean temperature of 17.7 °C, and a potential evapotranspiration of 900 mm, which strongly controlled the mobility of the pollutant into the soil. The soil moisture regime is xeric, and the soil temperature regime is thermic (USDA, 2003). The studied soil is a calcareous Regosol (FAO-ISRIC-ISSS, 1998) with scant development, sandy-loam texture (12% clay), low organic matter content ($< 2\%$), mean content in calcium carbonate equivalent of 130 mg g^{-1}, and pH close to 8.0 (Simón *et al.*, 1999).

To study the evolution in time of the oxidation processes of pyrite tailings covering the soils, a systematic sampling was made three years after the spill (Martín *et al.*, 2008). The soil was covered by a layer of tailing (2–5 cm thick) and showed a strong morphological differentiation in depth (Fig. 1). Just under the tailings, a light-greyish layer (2.5Y 7/2) appeared with a mean thickness of 5 mm, followed by a reddish-brown layer (10YR 5/6) with a mean thickness of 70 mm; below this depth, the soil appeared brown color (2.5Y 5/4) like the original unaffected soil.

A systematic sampling was made in a trial pit 1 m × 2 m and 0.8 m depth; sampling was carried out in triplicate on three of its walls. A sample was taken every 5 mm to a depth of 70 mm, then every

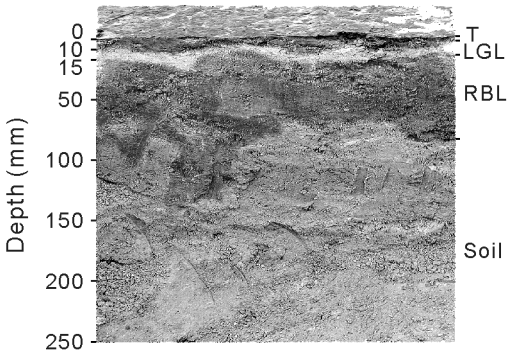

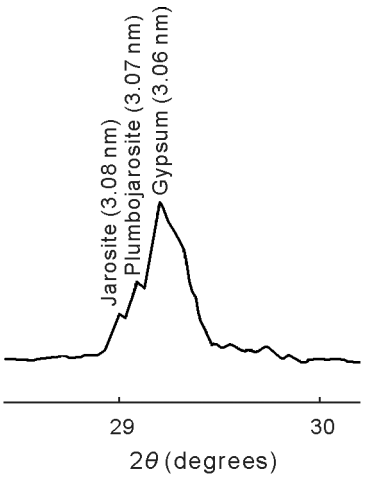

Fig. 1 General view of the soil covered by the pyrite tailings. T = tailings; LGL = light-greyish layer; RBL = reddish-brown layer.

Fig. 2 Detail of X-ray diffraction (XRD) diagram (between 29–30 degrees) of the light-greyish layer of soil.

10 mm to a depth of 120 mm, and finally, every 50 mm to a depth of 570 mm.

Soil samples were air-dried and sieved to 2 mm to calculate the percentage of gravels, and all the analyses were made with the fine earth fraction (< 2 mm). In soil samples, pH was determined potentiometrically in a 1:2.5 (soil:water) suspension; calcium carbonate content was measured by the method of Williams (1948), and gypsum content was determined by precipitation with acetone (Bower and Huss, 1948). Total content in major elements (Si_T, Al_T, Fe_T, and S_T) was determined after preparation of soil pellets using lithium tetraborate (0.6:5.5) by X-ray fluorescence in a Philips PW-1404 instrument, which is in the Research Instrumentation Center at the University of Granada. Free-iron oxides (Fe_d) were extracted using dithionite-citrate (Holmgren, 1967), and poorly crystallized iron oxides (Fe_o) were extracted using oxalic-oxalate (Schwertmann and Taylor, 1977) and both were measured by atomic absorption spectroscopy using a VARIAN SpectrAA 220FS instrument, which is in the Soil Science Department of the University of Granada. Crystallized iron forms (Fe_c) were considered as the difference between Fe_d and Fe_o; whereas iron forms associated with primary soil minerals (Fe_m) were estimated as the difference between Fe_T and Fe_d.

Total concentrations of arsenic and heavy metals were determined in finely ground soil samples (< 0.05 mm) after digestion in strong acids [HNO_3 (65%) + HF (40%)] in a ratio 2:3; meanwhile, the water-soluble forms were obtained from soil:water extracts in a ratio 1:10 using norma DIN 38414-S4 method. In each digested sample and aqueous extract obtained, the Cu, Zn, Cd, As, and Pb contents were measured by ICP-MS (inductively coupled plasma-mass spectrometry) using a PE Sciex ElAN-5000A spectrometer in the Research Instrumentation Center of the University of Granada. The accuracy of the method was corroborated by analyses (6 replicates) of standard reference material (SRM 2711) (Simón *et al.*, 2002). Statistical procedure was made using the package SPSS (ver.15.0).

RESULTS AND DISCUSSION

Alteration processes

The oxidation of pyrite tailings resulted in an intense alteration of the soil, causing important changes in morphological characteristics and degradation of the soil properties. One of the main effects was the strong acidification of the soil surface layer, with pH decreasing from values next to 8 in the unaffected soil to values next to 2 in the uppermost 15 mm (Table I). Simultaneously, carbonate minerals

dissolution was observed, being complete in the uppermost layer of the soil (0–35 mm) and partial until 100 mm (below 70 mm, the limit of the reddish-brown layer). The released calcium cations reacted with the sulfate ions of the acidic solution to form gypsum (Table I). The successive rains after three years produced the continuous alteration of the soil, even affecting more stable minerals as feldspars and phyllosilicates (Martín *et al.*, 2008).

TABLE I

pH, calcium carbonate content, and gypsum content in the affected soil

Depth[a)]	pH		$CaCO_3$		Gypsum	
	Mean	SD[b)]	Mean	SD	Mean	SD
mm			mg g^{-1}			
0–5	2.09	0.03	0.0	0.0	95.3	2.2
5–10	2.29	0.05	0.0	0.0	96.1	1.9
10–15	2.38	0.06	0.0	0.0	95.2	2.1
15–20	2.76	0.04	0.0	0.0	80.4	1.6
20–25	2.89	0.05	0.0	0.0	79.5	1.4
25–30	3.21	0.06	0.0	0.0	79.3	0.9
30–35	4.46	0.03	0.0	0.0	77.1	1.0
35–40	5.00	0.05	12.8	1.2	76.4	1.9
40–45	5.29	0.05	15.5	1.6	72.2	1.4
45–50	5.53	0.06	14.6	2.0	72.0	1.1
50–55	6.10	0.08	14.8	1.4	61.3	0.6
55–60	6.27	0.08	18.9	1.0	53.5	1.1
60–65	6.50	0.06	29.1	1.9	40.8	1.5
65–70	6.89	0.08	32.4	2.4	24.6	0.8
70–80	7.09	0.05	41.4	3.6	8.2	0.5
80–90	7.42	0.07	76.2	6.2	1.2	0.6
90–100	7.60	0.07	79.5	7.4	0.0	0.0
100–110	7.76	0.06	86.2	6.3	0.0	0.0
110–120	7.68	0.07	86.4	11.5	0.0	0.0
120–170	7.80	0.07	90.0	6.9	0.0	0.0
170–220	7.86	0.09	88.7	8.4	0.0	0.0
220–270	7.84	0.05	85.6	6.5	0.0	0.0
270–320	8.00	0.08	88.0	7.3	0.0	0.0
320–370	7.92	0.08	86.9	8.5	0.0	0.0
370–420	7.80	0.06	91.0	10.7	0.0	0.0
420–470	7.99	0.05	88.0	7.6	0.0	0.0
470–520	7.90	0.08	89.0	9.5	0.0	0.0
520–570	8.10	0.07	87.0	8.9	0.0	0.0

[a)]0–5 mm is a light-greyish layer; 5–70 mm is a reddish-brown layer.
[b)]Standard deviation

The oxidation of Fe^{2+} after the drying and aeration of the tailings caused the precipitation of Fe^{3+} into the soil, which accumulated the iron in the upper part of the soil and was mainly responsible for the reddish color. However, the successive infiltrations of acidic waters resulted in a redissolution of the iron precipitated in the uppermost 5 mm of the soil, and a subsequent infiltration to deeper depth, leading to the formation of a light-greyish layer in the soil just below the tailings. The distribution of the concentrations of total iron (Fe_T), iron extractable with ammonium oxalate (Fe_o), and iron extractable with dithionite-citrate (Fe_d) in different soil depths is shown in Table II. The Fe_d and Fe_o contents were significantly ($P < 0.05$) higher in the reddish-brown layer (up to 70 mm) than in the unaffected soil. In this sense, the Fe_d represents around 40%–50% of the Fe_T in the uppermost layer (< 35 mm), whereas its contents in the unaffected soil ranges from 10% to 15% of the Fe_T. Otherwise, the content of Fe_o represented around 25%–30% of the Fe_T in the uppermost layer (< 35 mm), but just 3%–4% in the unaffected soil. The ratio Fe_o/Fe_d can indicate the degree of crystallinity of the iron forms, the higher values were measured in the reddish-brown layer (mean 0.60), indicating the abundance of amorphous

iron forms; meanwhile this ratio decreased to 0.32 in the unaffected soil, where the crystalline forms dominate.

TABLE II

Concentrations of total iron (Fe_T), iron extracted with dithionite-citrate (Fe_d), iron extracted with oxalic-oxalate (Fe_o), total sulfur (S_T), sulfur precipitated as hydroxysulfates (S_{hs}), total silicon (Si_T) and total aluminium (Al_T) in the affected soil

Depth[a)]	Fe_T		Fe_d		Fe_o		S_T		S_{hs}		Si_T		Al_T	
	Mean	SD[b)]	Mean	SD	Mean	SD	Mean	SD	Mean	SD	Mean	SD	Mean	SD
mm	mg g^{-1}													
0–5	78.0	8.6	37.8	4.7	20.4	1.8	96.8	10.4	74.6	9.6	198.0	18.7	43.5	5.1
5–10	85.2	9.6	40.7	5.7	22.7	2.2	82.8	10.8	60.4	8.6	201.0	18.1	45.7	6.6
10–15	85.4	9.0	40.5	5.1	23.6	2.0	81.8	9.7	59.6	7.7	205.2	9.6	45.9	7.1
15–20	82.8	8.6	35.4	4.7	23.2	1.9	76.6	9.5	58.0	7.6	210.2	9.1	47.9	8.4
20–25	81.2	6.7	37.7	2.8	23.3	1.7	72.2	8.3	53.9	6.7	210.1	11.6	50.8	9.0
25–30	81.5	7.7	36.1	3.8	24.1	2.1	73.7	9.8	55.4	7.7	210.9	13.5	50.5	8.7
30–35	69.4	8.3	29.2	5.4	18.4	1.9	63.5	9.2	45.7	7.3	215.3	10.9	53.7	8.9
35–40	67.8	8.0	25.1	4.1	15.4	1.8	61.1	8.8	43.5	7.0	225.0	10.2	56.1	7.2
40–45	67.0	7.4	23.8	3.5	14.9	1.9	56.3	7.3	39.5	5.4	237.1	12.1	60.8	6.2
45–50	58.3	8.3	17.2	4.4	10.1	2.0	56.2	6.3	39.4	4.3	237.9	13.8	64.2	6.7
50–55	49.1	8.8	12.1	4.9	7.1	1.7	39.0	5.5	24.7	3.8	251.1	10.6	67.0	6.0
55–60	45.5	7.1	10.0	3.2	5.5	1.9	36.8	4.0	24.4	2.1	260.9	12.3	68.8	7.7
60–65	44.2	7.6	8.0	2.7	4.2	1.8	24.7	4.4	15.5	2.6	266.9	9.5	71.5	5.6
65–70	40.9	7.4	7.2	1.5	3.6	1.2	17.8	3.6	12.3	2.4	297.5	12.3	70.8	8.6
70–80	37.1	7.0	5.3	1.1	2.3	1.0	7.8	3.0	5.9	2.0	299.8	14.1	70.0	9.6
80–90	36.4	6.3	4.3	1.4	1.6	0.6	1.8	0.9	1.5	0.3	305.7	16.0	69.1	7.3
90–100	35.9	6.6	3.7	1.7	1.5	0.6	1.5	0.2	1.5	0.4	305.6	8.5	67.7	7.5
100–110	36.7	6.4	3.6	1.5	1.5	0.8	1.5	0.3	1.5	0.6	309.6	10.7	65.8	5.8
110–120	35.6	6.3	3.5	1.2	1.4	0.5	1.4	0.4	1.4	0.1	306.5	12.3	65.1	8.0
120–170	35.8	6.1	3.5	1.2	1.2	0.7	1.5	0.3	1.6	0.4	293.4	11.9	66.0	4.1
170–220	36.2	6.4	3.4	1.5	1.1	0.5	1.6	0.3	1.6	0.1	296.2	15.2	66.6	6.9
220–270	36.8	5.9	3.9	1.5	1.3	0.6	1.5	0.2	1.5	0.4	294.4	12.3	65.5	5.7
270–320	36.0	6.0	3.6	1.1	1.2	0.5	1.5	0.5	1.7	0.2	292.9	8.3	64.1	8.5
320–370	36.3	5.6	3.7	1.7	1.1	0.7	1.7	0.3	1.7	0.4	291.3	11.4	65.1	6.9
370-420	37.0	6.4	3.9	1.5	1.3	0.4	1.7	0.3	1.6	0.1	198.0	14.7	43.5	6.6
420–470	35.8	6.1	3.6	1.4	1.1	0.5	1.6	0.2	1.5	0.3	201.0	13.0	45.7	7.5
470–520	36.2	6.2	3.3	1.0	1.2	0.6	1.5	0.4	1.7	0.2	205.2	9.7	45.9	4.9
520–570	36.5	6.0	3.5	1.4	1.1	0.5	1.6	0.3	1.7	0.2	210.2	12.1	47.9	6.9

[a)] 0–5 mm is a light-greyish layer; 5–70 mm is a reddish-brown layer.
[b)] Standard deviation.

Alteration processes can also be observed in the neoformation of minerals in the soil profile. The presence of these minerals was notablein the scanning electron microscope (SEM) study and in the mineralogical analysis by XRD for these samples (Martín *et al.*, 2008). The gypsum precipitated at the initial stages is redissolved in the uppermost part of the soil due to the continuous infiltration of acidic waters coming from the tailing oxidation. The percentage of sulfur precipitated as hydroxysulfate (S_{hs}), which was obtained as the difference between the total sulfur (S_T) and that precipitated as gypsum (S_Y), *i.e.*, $S_{hs} = S_T\ S_Y$, reached values up to 66%–74% of the S_T within the reddish layer, decreasing with depth, where gypsum obtained from leaching was accumulated (Table II). The other neoformed minerals in soil were related to the iron and sulfates obtained from the acidic solution. These minerals belong mainly to the jarosite-group (Fig. 2), although others like schwertmannite and ferrihydrite have been abundantly described in this medium (Filipek *et al.*, 1987; Bigham *et al.*, 1996; Bigham and Nordstrom, 2000).

The ratio Fe_T/S_{hs} in the affected part of the soil resulted in values close to 1 within the light-grey layer (0–5 mm), values of 1.5 (similar ratio to the jarosite) in the reddish layer up to 50 mm depth, and

values between 2 and 3.3 in the bottom of the reddish layer (50–70 mm), the latter could be related to the presence of minerals with higher Fe/S ratio such as schwertmannite and ferrihydrite.

This alteration process also affected Si and Al, which were partially leached from the upper part of the alteration layer and accumulated as deep as 370 mm (out of the visible limit of the reddish layer). The maximum accumulation occurred between 60–90 mm for Al and between 90–120 mm for Si (Table II), indicating a higher mobility of silicon in relation to aluminium in this type of environment, which should be related to the pH and the different values of pK of these elements.

Mobility of Pollutant Elements

Arsenic had a low mobility in this medium, which caused its accumulation in the upper part of the soil. The continuous leaching of the acidic solution as a result of the pyrite-tailing oxidation caused strong variations of this element in depth by decreasing the arsenic concentration in the first 5 mm (light-grey layer) and reaching the maximum value (1 239 mg kg^{-1}) between 5 and 10 mm depth (Fig. 3).

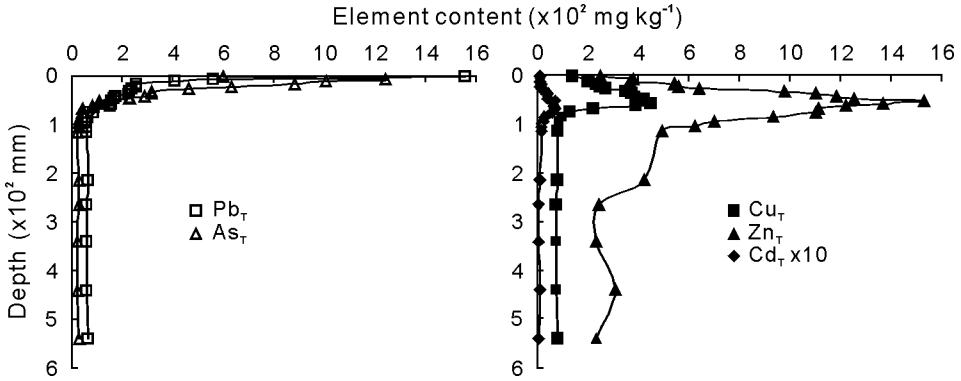

Fig. 3 Vertical distribution of total lead (Pb_T), arsenic (As_T), copper (Cu_T), zinc (Zn_T), and cadmium (Cd_T) in the affected soil.

In relation to the soil constituents, only a significant correlation between total arsenic (As_T) and total iron concentration (Fe_T) was found (Fig. 4), indicating that arsenic is likely to be adsorbed as H_2AsO^- by iron precipitated forms.

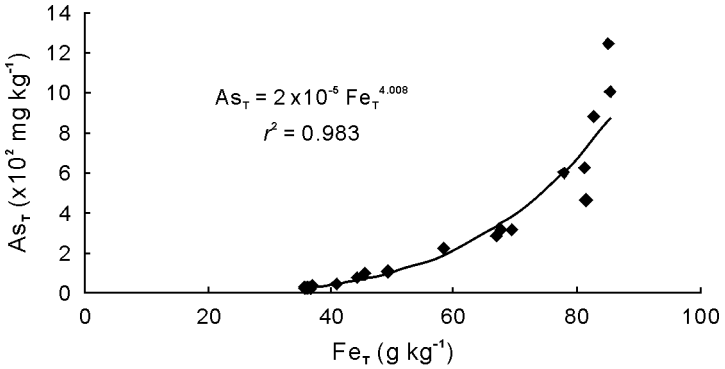

Fig. 4 Regression plot between total arsenic (As_T) and total iron concentration (Fe_T).

Otherwise, the correlation between the As_T and the different iron forms indicates the following regression equation:

$$As_T = 1.68Fe_o + 60.07Fe_c - 4.35Fe_m \quad (r^2 = 0.862) \tag{2}$$

Equation 2 suggested that three years after the spill, the adsorption of arsenic by crystallized iron

forms (Fe_c) was 35 times higher than the arsenic concentration precipitated with amorphous iron forms (Fe_o), whereas the iron linked to primary minerals (Fe_m) did not show any influence in arsenic mobility. Therefore, arsenic retention in these media should be related to the neoformation of iron hydroxysulfates (jarosite [$KFe_3SO_4(OH)_6$] and schwertmannite [$Fe_8O_8(OH)_6SO_4$] type minerals) and ferrihydrite ($5Fe_2O_3{\cdot}9H_2O$), suggesting that the removal of arsenic through coprecipitation and adsorption reactions is likely the dominant solid-phase control on the mobility of arsenic (Bigham *et al.*, 1996; Dold, 2003; Sánchez España *et al.*, 2005). In this way, the retention of arsenic was directly correlated to the Fe/S ratio, increasing the arsenic solubility in the upper part of the soil (Fig. 5), where the Fe/S ratio was lower, and the dissolution of iron-rich minerals occurred under acidic conditions (Al-Abed *et al.*, 2007). The distribution of the iron hydroxysulfates and oxyhydroxides in depth indicated an increase in the Fe/S ratio with depth, which was related to the decrease of jarosite and the increase in iron-rich minerals (schwertmannite and ferrihydrite). The retention of arsenic in relatively stable forms by ferrihydrite and schwertmannite is related to the reduction of soluble arsenic concentrations. (Carlson *et al.*, 2002; Courtin-Nomade *et al.*, 2003).

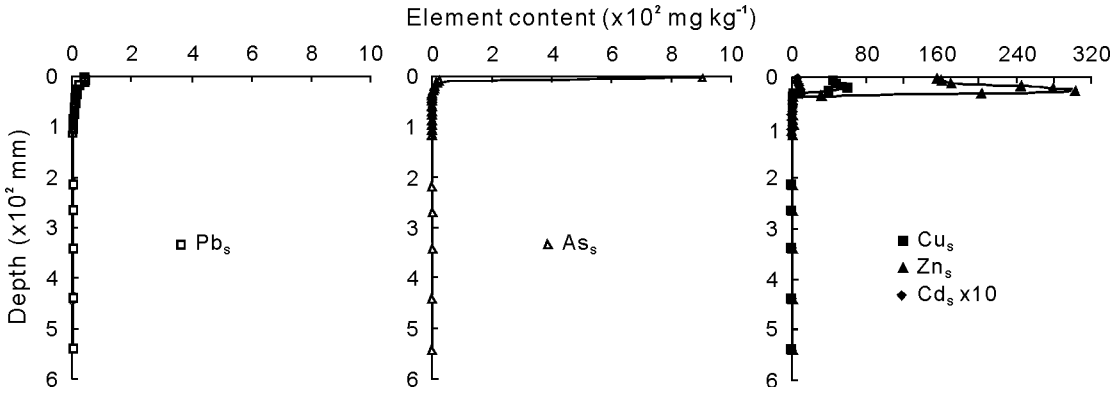

Fig. 5 Vertical distribution of water-soluble lead (Pb_S), arsenic (As_S), copper (Cu_S), zinc (Zn_S), and cadmium (Cd_S) in the affected soil.

Lead is the element with less mobility, tending to accumulate in the upper part of the soil and reaching concentrations above 1 500 mg kg^{-1} in the uppermost millimeters (Fig. 3). A significant correlation ($P < 0.001$) between total lead content (Pb_T), total iron content (Fe_T), and sulfates that do not form gypsum (S_{hs}) was found. This relationship was established as follows,

$$S_{hs} = -3.081 + 10.275Pb_T + 0.948Fe_T \quad (r^2 = 0.959) \tag{3}$$

suggesting that the neoformation of Pb-hydroxysulfates was one of the main processes involved in the precipitation of this metal; in this way, the presence of plumbojarosite ($PbFe_6(SO_4)_2(OH)_{12}$) has been detected by X-Ray diffraction in the uppermost millimeters of the soil. Otherwise, the concentration of Pb^{2+} and sulphate ions in the soil solution and their over-saturation in relation to anglesite ($PbSO_4$) indicated that lead might also precipitate in this mineral form (Fig. 6).

The higher concentrations of water-soluble lead (Pb_s) were also found in the uppermost 15 mm of the soil (Fig. 5), with values above 0.42 mg kg^{-1}; in this case, Pb_s presented significant ($P < 0.01$) and direct correlation with Pb_T (0.779) and inverse correlation with pH (−0.898). Anyway, despite the high Pb concentration in this part of the soil, the soluble forms (Pb_s) only represent between 0.11%–0.03% of the total Pb; therefore, the Pb fixation could be controlled by the precipitation and stability of plumbojarosite in acidic conditions (Sastre *et al.*, 2004)

Zinc and cadmium mobility and distribution in soil depth is strongly controlled by pH conditions. These elements tended to be leached from the upper part of the soil and to accumulate in depth, reaching higher concentrations when pH values ranged from 5 to 7. At pH 6.1 (between 50 and 55 mm depth),

Zn concentrations had a maximum value exceeding 1 500 mg kg^{-1}, whereas Cd reached a value of 7 mg kg^{-1} (Fig. 3). In addition, the maximum Zn and Cd water soluble concentrations (Zn_s and Cd_s, respectively) occurred between 25–35 mm depth (Fig. 5), where the pH value of the soil was below 4.5 (Table I).

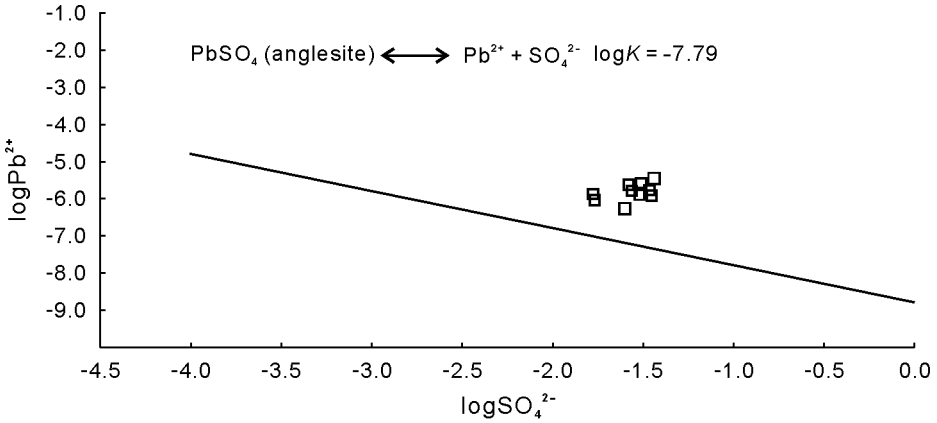

Fig. 6 Over-saturation of the samples of the alteration layer in relation to the equilibrium equation of anglesite.

When we correlated total zinc and cadmium concentrations (Zn_T and Cd_T) with soil properties, the only significant correlation ($P < 0.01$) was obtained with total aluminium and silicon (Al_T and Si_T), as shown by the regression equation:

$$Zn_T = -989.29 + 66.22\ Al_T - 8.25\ Si_T \quad (r^2 = 0.981) \tag{4}$$

$$Cd_T = -6.907 + 0.317\ Al_T - 0.033\ Si_T \quad (r^2 = 0.859) \tag{5}$$

Equations 4 and 5 suggested that precipitated aluminium forms mainly controlled zinc and cadmium precipitation, as has been previously reported by some authors (Micera *et al.*, 1986; Keizer and Bruggenwert 1991; Zachara *et al.*, 1992). On the other hand, the negative correlation between Zn_T and Cd_T with silicon (Si_T) could be associated with the coprecipitation process between silicon and aluminium in the ground-mass of the soil, which may lead to a reduction in aluminium adsorption capacity.

Copper showed a distribution similar to that of Zn and Cd, with some differences. Concentrations of copper were also related to pH, decreasing in the upper centimeters of the soil and increasing with depth (Fig. 3). Total concentrations (Cu_T) had a maximum value of 420 mg kg^{-1} occurring between pH 4.5–6.5 (at 45–50 mm depth). The water-soluble forms (Cu_s) indicated a lower range of mobility than in the case of zinc and cadmium (Fig. 5), being the maximum concentration of Cu_s between 20–25 mm depth, which coincides with the part of the soil with pH < 3.5.

The relation of copper with the soil constituents showed a significant correlation ($P < 0.01$) between Cu_T, Al_T, and S_{hs}, as represented in the following equation:

$$Cu_T = -860.46 + 18.45\ Al_T + 3.21\ S_{hs} \quad (r^2 = 0.856) \tag{6}$$

indicating that Al precipitation and neoformation of hydroxysulfate minerals were the main components controlling the mobility of copper in soil. In the case of iron hydroxysulfates, we included Cu_T in the regression analysis of Eq. 3, obtaining an increase in the correlation coefficient:

$$S_{hs} = -34.208 + 0.918Fe_T + 10.856Pb_T + 28.512Cu_T \quad (r^2 = 0.974) \tag{7}$$

Therefore, we could observe the high significant relation between iron hydroxysulfates and the retention of lead and copper in this type of soil.

CONCLUSIONS

The oxidation of pyrite tailings deposited over a carbonate soil during three years resulted in an intense alteration process, causing important changes in morphological characteristics and degradation of the main soil properties.

The mobility of arsenic, lead, zinc, cadmium, and copper was strongly affected by the mineralogical changes and neoformations that occurred in the soil, and, in some cases, by the change in pH conditions. Arsenic retention was strongly related to coprecipitation and adsorption reactions caused by the neoformation of iron hydroxysulfates and oxyhydroxides (mainly jarosite, schwertmannite and ferrihydrite), indicating a higher stability of arsenic retention with the increase in the Fe/S ratio of the minerals. Lead precipitation was related to the neoformation of plumbojarosite in the uppermost part of the soil, and possibly, to the formation of anglesite in other parts of the alteration layer. Zinc and cadmium showed higher mobility in this soil, but under the climatic conditions, the intense leaching during three years of these metals has only affected the first 30 cm of the soil; the precipitation of these elements was directly related to pH and to the coprecipitation of amorphous aluminium forms in the ground-mass of the soil. Finally, copper mobility was also related to pH, but the mobility range was lower than that in the case of zinc and cadmium; and the retention of copper in this soil was directly related to the coprecipitation of amorphous aluminium forms and also to the neoformation of iron oxyhydroxysulfates.

ACKNOWLEDGMENT

We thank Dr. David Nesbitt in USA and Dr. Ana Palomares in Spain for correcting the English version of the manuscript.

REFERENCES

Al-Abed, S. R., Jegadeesan, G., Purandare, J. and Allen, D. 2007. Arsenic release from iron rich mineral processing waste: Influence of pH and redox potential. *Chemosphere.* **66**(4): 775–782.

Bigham, J. M. and Nordstrom, D. K. 2000. Iron and aluminum hydroxysulfates from acid sulfate waters. *In* Alpers, C. N., Jambor, J. L. and Nordstrom, D. K. (eds.) Sulfate Minerals: Crystallography, Geochemistry and Environmental Significance. Reviews in Mineralogy and Geochemistry. Vol. 40. Mineral Soc. Amer. Geochem. Soc. pp. 351–403.

Bigham, J. M., Schwertmann, U., Traina, S. J., Winland, R. L. and Wolf, M. 1996. Schwertmannite and the chemical modelling of iron in acid sulphate waters. *Geochim. Cosmochim. Ac.* **60**(12): 2 111–2 121.

Bower, C. A. and Huss, R. B. 1948. Rapid conductometric method for estimating gypsum in soils. *Soil Sci.* **141**: 99–204.

Carlson, L., Bigham, J. M., Schwertmann, U., Kyek, A. and Wagner, F. 2002. Scavenging of As from acid mine drainage by schwertmannite and ferrihydrite: A comparison with synthetic analogues. *Environ. Sci. Technol.* **36**: 1 712–1 719.

Courtin-Nomade, A., Bril, H., Neel, C. and Lenain, J. 2003. Arsenic in iron cements developed within tailings of a former metalliferous mine—Enguiales, Aveyron, France. *Appl. Geochem.* **18**: 395–408.

Cravotta III, C. A. and Trahan, M. K. 1999. Limestone drains to increase pH and remove dissolved metals from acidic mine drainage. *Appl. Geochem.* **14**: 581–606.

Dold, B. 2003. Dissolution kinetics of schwertmannite and ferrihydrite in oxidized mine samples and their detection by differential X-ray diffraction (DXRD). *Appl. Geochem.* **18**: 1 531–1 540.

Dorronsoro, C., Martín, F., Ortíz, I., García, I., Simón, M., Fernández, E., Aguilar, J. and Fernández, J. 2002. Migration of trace elements from pyrite tailings in carbonate soils. *J. Environ. Qual.* **31**: 829–835.

FAO-ISRIC-ISSS. 1998. World Reference Base for Soil Resources. FAO, Roma.

Filipek, L. H., Nordstrom, D. K. and Ficklin, W. H. 1987. Interaction of acid mine drainage with waters and sediments of West Squaw Creek in the West Shasta Mining District, California. *Environ. Sci. Technol.* **21**: 388–396.

Holmgren, G. G. S. 1967. A rapid citrate-dithionite extractable iron procedure. *Soil Sci. Soc. Am. Proc.* **31**: 210–211.

Holub, Z., Šimonovičová, A. and Banásová, V. 1993. The influence of acidification on some chemical and microbiological properties of soil, determining plant viability. *Biol. Bratislava.* **48**(6): 671–675.

Förstner, U. and Wittmann, G. T. W. 1983. Metal Pollution in the Aquatic Environment. Springer-Verlag, Berlín.

Karathanasis, A. D. and Thompson, Y. L. 1995. Mineralogy of iron precipitates in a constructed acid mine drainage wetland. *Soil Sci. Soc. Am. J.* **54**: 1 773–1 781.

Karathanasis, A. D., Evangelou, V. P. and Thompson, Y. L. 1988. Aluminium and iron equilibria in soil solutions and surface waters of acid mine watersheds. *Environ. Qual.* **19**: 534–543.

Keizer, P. and Bruggenwert, M. G. M. 1991. Adsorption of heavy metals by clay-aluminium hydroxide complexes. *In* Bolt, G. H. (ed.) Interactions at the Soil Colloid-Soil Solution Interface. Kluwer Academic Publishers. Dordrecht. pp. 177–203.

Lacey, E. T. and Lawson, F. 1979. Kinetics of the liquid-phase oxidation of acid ferrous sulfate by the bacterium Thiobacillus ferroxidans. *Biotechnol. Bioeng.* **12**: 29–50.

Martín, F., García, I., Díez, M., Sierra, M., Simón, M. and Dorronsoro, C. 2008. Soil alteration by continued oxidation of pyrite tailings. *Appl. Geochem.* **23**: 1 152–1 165.

Micera, G., Gessa, C., Melis, P., Premoli, A., Callocchio, R. Y. and Deiana, S. 1986. Zinc (II) adsorption on aluminium hydroxide. *Colloid. Surface.* **17**: 389–394.

Monterroso, M. C. and Macías, F. 1998. Immobilization process of trace elements in acid mine water. *Edafología* (in Spanish). **5**: 59–70.

Nordstrom, D. K. 1982. Aqueous pyrite oxidation and the consequent formation of secondary iron minerals. *In* Kitrick, J. A., Fanning, D. S. and Hossner, L. R. (eds.) Acid Sulfate Weathering. Soil Science Society of America. Madison, WI. pp. 37–56.

Nordstrom, D. K. and Alpers, C. N. 1999. Geochemistry of acid mine waters. *In* Plumlee, G. S. and Logsdon, M. J. (eds.) The Environmental Geochemistry of Mineral Deposits. Part A. Processes, Techniques, and Health Issues. Society of Economic Geologists, Inc. pp. 133–160.

Sánchez España, J., López Pamo, E., Santofimia, E., Aduvire, O., Reyes Andrés, J. and Barettino, D. 2005. Acid mine drainage in the Iberian Pyrite Belt (Odiel river watershed, Huelva, SW Spain): Geochemistry, mineralogy and environmental implications. *Appl. Geochem.* **20**: 1 320–1 356.

Sastre, J., Hernández, E., Rodríguez, R., Alcobé, X., Vidal, M. and Rauret, G. 2004. Use of sorption and extraction tests to predict the dynamics of the interaction of trace elements in agricultural soils contaminated by a mine tailing accident. *Sci. Total Environ.* **329**: 261–281.

Schwertmann, U. and Taylor, R. M. 1977. Iron oxides. *In* Dixon, J. B. and Webb, S. B. (eds.) Mineral in Soil Environments. Soil Science Society of America, Madison. pp. 148–180.

Simón, M., Dorronsoro, C., Ortíz, I., Martín, F. and Aguilar, J. 2002. Pollution of carbonate soils in a Mediterranean climate due to a tailings spill. *Eur. J. Soil Sci.* **53**: 1–10.

Simón, M., Martín, F., Ortíz, I., García, I., Fernández, J., Fernández, E., Dorronsoro, C. and Aguilar, J. 2001. Soil pollution by oxidation of tailings from toxic spill of a Pyrite mine. *Sci. Total Environ.* **279**: 63–74.

Simón, M., Ortíz, I., García, I., Fernández, E., Fernández, J., Dorronsoro, C. and Aguilar, J. 1999. Pollution of soils by the toxic spill of a pyrite mine (Aznalcóllar, Spain). *Sci. Total Environ.* **242**: 105–115.

Singer, P. C. and Stumm, W. 1970. Acid mine drainage: The rate determining step. *Science.* **167**: 1 121–1 123.

Stumm, W. and Morgan, J. J. 1981. Aquatic Chemistry: An Introduction Emphasizing Chemical Equilibria in Natural Waters. John Wiley & Sons, New York.

United States Department of Agriculture (USDA). 2003. Keys to Soil Taxonomy. Soil Survey Staff. 9th Edition. United States Department of Agriculture, Washington.

Williams, D. E. 1948. A rapid manometric method for the determination of carbonate in soils. *Soil Sci. Soc. Am. Proc.* **13**: 127–129.

Xu, Y., Schwartz, F. W. and Traina, S. J. 1997. Treatment of acidic-mine water with calcite and quartz. *Environ. Eng. Sci.* **14**(3): 141–152.

Zachara, J. M., Smith, S. C., Resch, C. T. and Cowan, C. E. 1992. Cadmium sorption to soil separates containing layer silicates and iron and aluminium oxides. *Soil Sci. Soc. Am. J.* **56**: 1 074–1 084.